Proposal for J-PARC 30-GeV Proton Synchrotron

Measurement of displacement cross-section of proton of 8 and 30 GeV for high-intensity proton accelerator facilities

Dec 19, 2017

S. Meigo, S. Hasegawa, Y. Iwamoto, H. Iwamoto, H. Matsuda, and F. Maekawa

J-PARC Center, Japan Atomic Energy Agency (JAEA) Japan

M. Yoshida, T. Nakamoto, S. Makimura, and T. Ishida

J-PARC Center, High Energy Accelerator Research Organization (KEK), Japan

Executive Summary

For estimation of damage such as beam window and target material used at the accelerator facility, displacement per atom (DPA) is widely employed as an index of the damage. The DPA is estimated by the particle flux multiplied displacement cross-section, which is obtained by calculation based on intra-nuclear cascade model. Although the DPA is widely employed, the experimental data of displacement cross-section are scarce for a proton in the energy region above 20 MeV. In the recent study of the displacement cross-section, it was reported that the displacement cross-section of tungsten has 8 times difference among the calculation models. To obtain experimental data, some of our group has measured the displacement cross-section of copper for 125-MeV proton at Kyoto University. The displacement cross-section can be easily obtained by observing the change of resistivity of the sample cooled by a cryocooler to sustain the damage of the target.

In this study aiming to improve the calculation model, the displacement cross-section is measured. The proton with the kinetic energy of 8 GeV and 30 GeV irradiates the sample, which is contained in the vacuum chamber placed at upstream of the Main Ring (MR) abort beam dump. Based on the previous experiment, the requirement of the accumulated intensity is found to be very low such as $5x10^{14}$ for each experiment, which used a thin sample. Therefore, the requirement beam time for the present experiment is concise and the residual radiation dose will be low.

The budget for the present proposed experiment was already obtained from Ministry of education, culture, sports science and technology Japan (MEXT). The similar experiment will be carried out by our group at the beam dump placed at exit channel of the 3-GeV synchrotron in J-PARC, to obtain the displacement cross-section in the energy region from 0.4 GeV to 3 GeV. Also, the similar experiment will be carried out at RCNP to acquire the experimental data less than 400 MeV. Thus, in the vast energy range, the displacement cross-section can be obtained for the proton, which will help to improve the damage estimation of the target material and superconducting magnet for the high power accelerator facilities.

Contents

1. Purpose and background

1.1 Introduction

As the power of accelerators is increasing, the prediction of the structural damage to materials under irradiation is essential for the design [1]. To decrease hazard of the radioactive waste produced in a nuclear reactor, Japan Atomic Energy Agency (JAEA) proposes the Accelerator Driven System (ADS) with extremely high power accelerator such as 30 MW with proton having a kinetic energy about 1.5 GeV. A lead-bismuth eutectic (LBE) is one of a candidate of the target, which simultaneously plays the role of the coolant. In the design of the ADS, damage to the window material is one of a critical issue. In J-PARC, Transmutation Experimental Facility (TEF) is planned to build for the study of the target material for the ADS.

Beam windows play essential roles in high-power proton accelerator facilities. At Material Life science experimental Facility (MLF) in J-PARC, an aluminum alloy is utilized as beam window separating between high vacuum area and target station. The T2K collaboration uses the titanium alloy as the beam window. To operate high power accelerator with confidence, the damage estimation of the target material is essential.

For the quantitative specification of the damage to the target material, displacement per atom (DPA) is employed in general, which is widely used for the estimation of damage nuclear reactor and fusion reactor. Typically, the characterization of the material is estimated by the post-irradiation examination (PIE). The particle flux estimates multiplied displacement cross-section gives the DPA. In the lower energy region less than 20 MeV, the displacement cross-section for charged particles can predict well because Coulomb scattering mainly causes the displacement. For the neutron in lower energy, the DPA can be estimated with reasonable accuracy as well, based on elastic scattering and inelastic scattering, in which the cross-section and outgoing energy of the second particle are well known, The calculation method of displacement cross-section has been established for the low-energy regions where nuclear reactions do not produce secondary particles.

However, for the particles in high energy region, the experimental data of displacement cross-section are so scarce that the calculated displacement cross-section

has not been investigated for the high-energy regions, and the accuracy of the calculation method of displacement cross-sections was unknown. For the neutron and charged particle in the energy region above 20 MeV, many reaction channels open to produce secondary particle. In order to obtain displacement cross-section above 20 MeV, the calculation codes such as PHITS, MARS, FLUKA, and MCNPX based on the intra-nuclear cascade model are utilized. Figure 1 shows the displacement cross-sections calculated by Mokov with the MARS using several models [2] compared with the experimental data. Mokov reported that the displacement cross-section of tungsten has 8 times difference in various calculation models. It should be noted that 8 times of ambiguity for the displacement cross-section makes 8 times ambiguity of lifetime estimation for target materials. For validation and improvement of the estimation of the DPA, the experimental data are crucial. However, the experimental data of the DPA are scarce, and there are five experimental data for displacement cross-section in the proton energy region above 20 MeV. For improvement of the displacement cross-section, the experimental data are required.

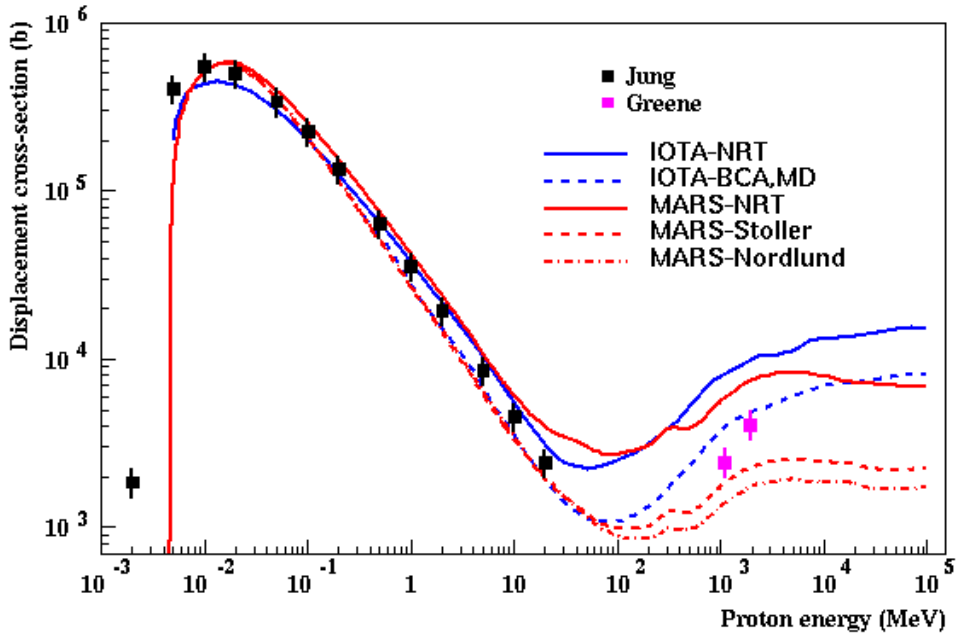

Fig. 1: Comparison of displacement cross-section of tungsten between experiment and calculation with MARS by using various damage models [2].

As the increase of the beam power, radiation damage of superconducting magnet is an issue. In J-PARC, the COMET experiment (J-PARC E21) is planned to search for the coherent neutrinoless transition of a muon to an electron in a muonic atom (μ−e conversion). The superconducting solenoid will be utilized to capture pion from the production target with high-efficiency.

1.2 Calculation of DPA

DPA is defined by the integral of displacement cross-section $\sigma_{\text{disp.}}$ and accumulated particle flux $\phi(E)$ as shown Eq. (1).

$$DPA = \int \sigma_{\text{disp.}}(E)\phi(E)dE \quad (1),$$

where E is the kinetic energy of irradiation particles. The displacement cross-section is defined as following equations.

$$\sigma_{\text{disp-cal.}} = \sum_i \int_{E_d}^{T_i^{\max}} d\sigma/dT_i \quad (2),$$

where $d\sigma/dT_i$ is recoil atom kinetic energy distribution, T is the kinetic energy of recoil particle i, N_{NRT} is the number of defects (Frenkel pairs) which is defined as a vacancy and a self-interstitial atom in the irradiated material using the Norgertt–Robinson–Torrens (NRT) approximation [3], which has been widely used from that time. η is the defect production efficiency [4].

1.3 Measurement of displacement cross-section at KURRI

Experimental displacement cross-sections are needed to validate DPA values calculated with Monte Carlo codes for lifetime estimation of devices at the ADS Target Test Facility (TEF-T) in J-PARC (400 MeV protons) [5], IFMIF (40 MeV deuteron) [6], and so on. However, there were no experimental displacement cross-sections in the energy region lower than 20 MeV, except for data for 1.1 and 1.94 GeV proton irradiation of copper and tungsten obtained at the Brookhaven National Laboratory (BNL) [7]. The experimental displacement cross-section is related to the defect-induced electrical resistivity changes as follows [8].

$$\sigma_{disp-\exp} = \frac{1}{\rho_{FP}} \frac{\Delta\rho_{metal}}{\phi} \quad (3).$$

Where $\Delta\rho_{metal}$ is the electrical resistivity increase (Ωm) which is the sum of resistivity per Frenkel pair and ϕ is the accumulated proton beam flux (/m^2). Damage rate (Ωm^3) is defined as $\Delta\rho_{metal}/\phi$. ρ_{FP} (Ωm) is the Frenkel-pair resistivity which was derived from damage rate measurements in single crystals under electron irradiation at low temperature and given by literature [4,9]. The number of defects is experimentally related to defect-induced changes in the electrical resistivity of metals at cryogenic temperature (around 10 K), where recombination of Frenkel pairs by thermal motion is well suppressed [6, 9 and 10].

In the BNL experiments [7], the cryostat assembly for sample irradiation consisted of a complicated cryogenics system to deliver a metered flow of liquid cryogen (liquid nitrogen and liquid helium) for controlling the sample temperature. To measure the damage rate $\Delta\rho_{metal}/\phi$ using various beams without a complicated cryogenic system in accelerator facilities, we have developed a cryogen-free cooling system using a Gifford–McMahon (GM) cryocooler in the beam line of the Fixed-Field Alternating Gradient (FFAG) accelerator facility at Kyoto University Research Reactor Institute (KURRI) [12] as shown in Fig. 2 [13]. Note that beam energy and intensity (125 MeV and 1nA) are fixed at FFAG accelerator facility. The sample was a copper wire with a 250-μm diameter and 99.999 % purity sandwiched between two aluminum nitride ceramic sheets as shown in the right side of Fig. 3.

The electrical resistivity changes of the copper wire were measured using the four-probe technique. After 125 MeV proton irradiation with 1.45×10^{18} protons/m^2 (20 hours, 1 nA) at 12 K, the total resistivity increase was 4.94×10^{-13} Ωm (resistance increase: 1.53 μΩ). The resistivity increase did not change during annealing after irradiation below 15 K. Figure 4 shows the experimental displacement cross-section of copper in our work [13] and previous studies [7]. The experimental data at 125 MeV irradiation shows similar results to the experimental data for 1.1 and 1.94 GeV. Comparison with the PHITS and revised radiation damage model [14,15] gives a good quantitative description of the displacement cross-section in the energy region >100 MeV although the calculated results with SRIM code [16] (dashed line) are much smaller than the experimental data due to lack of the secondary particles produced by nuclear reactions.

The increase in electrical resistivity due to high-energy protons provides straightforward information such as degradation of the stabilizer of the superconductor, which compromises quench protection and increases magnetothermal instability [17], for the superconducting accelerator magnet in the High Luminosity Large Hadron Collider [18] and the Future Circular Collider [19].

Taking into consideration of these results, we have launched a comprehensive study of the radiation damage in metals (aluminum, copper, tungsten) under proton irradiation. Our final goal is to create data libraries of displacement cross-sections using PHITS with an energy range from 0.1 to 30 GeV. It will be necessary to validate the model mentioned above based on measurements of damage rates using our cryogenic devices developed in KURRI.

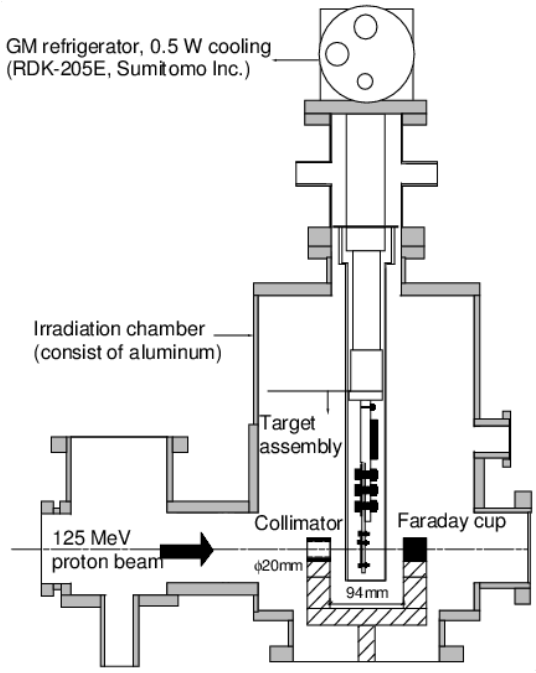

Fig. 2: Schematic of the irradiation chamber developed in the beamline at FFAG accelerator facility in Kyoto University Research Reactor Institute (KURRI) [13].

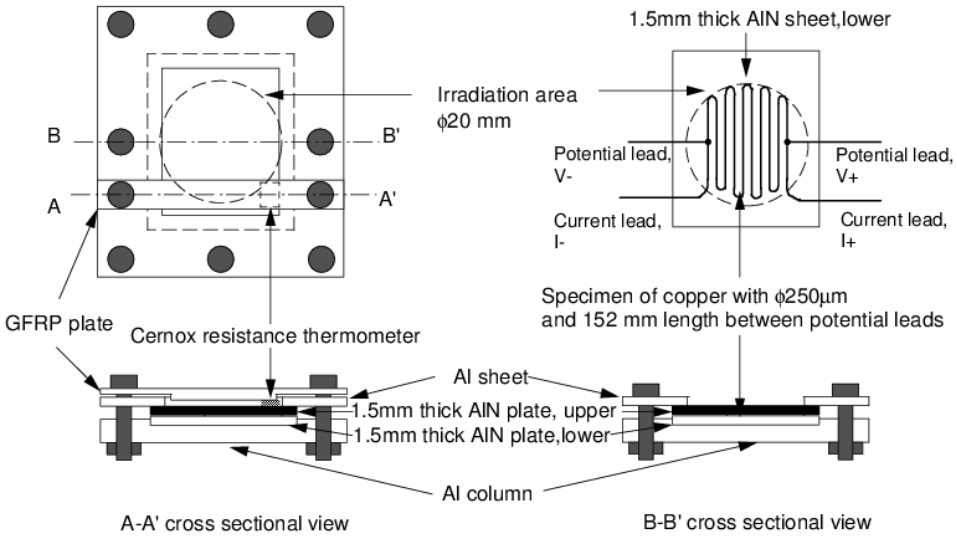

Fig. 3: Drawing of the sample and its retention developed in the beamline at FFAG accelerator facility in KURRI [13].

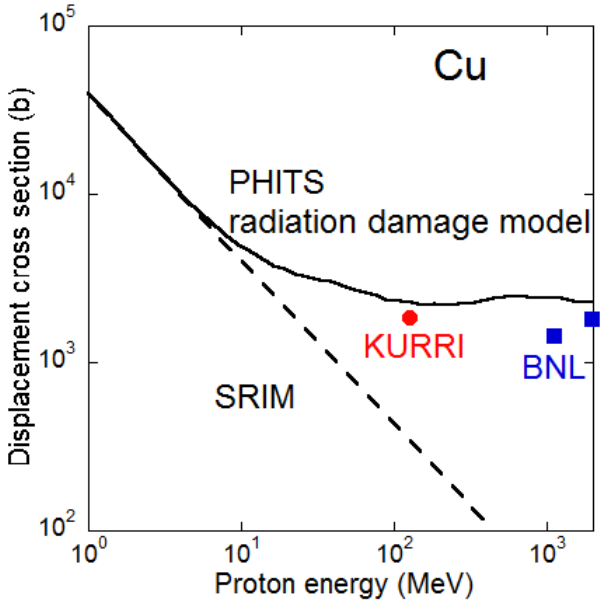

Fig. 4: Displacement cross-sections for proton irradiation of copper: our group work [13] (red circle), from the BNL data [7] (blue squares), the cross-section calculated using the PHITS-radiation damage model [15] (solid line), and SRIM code [16] (solid dashed line).

1.4 Measurement of displacement cross-section at RCNP

By some of our group, the similar experiment for the proton energy less than 0.4 GeV has started at Research Center for Nuclear Physics (RCNP) of Osaka University. The experiment has been already approved by the BPAC at RCNP and was carried in this fiscal year. Figure 5 shows the vacuum chamber utilized in the experiment carried out for the proton with the kinematic energy of 200 MeV in November 2017. As samples of the experiment, aluminum and copper were utilized. At RCNP, the kinematic energy of projectile proton 400 MeV is planned.

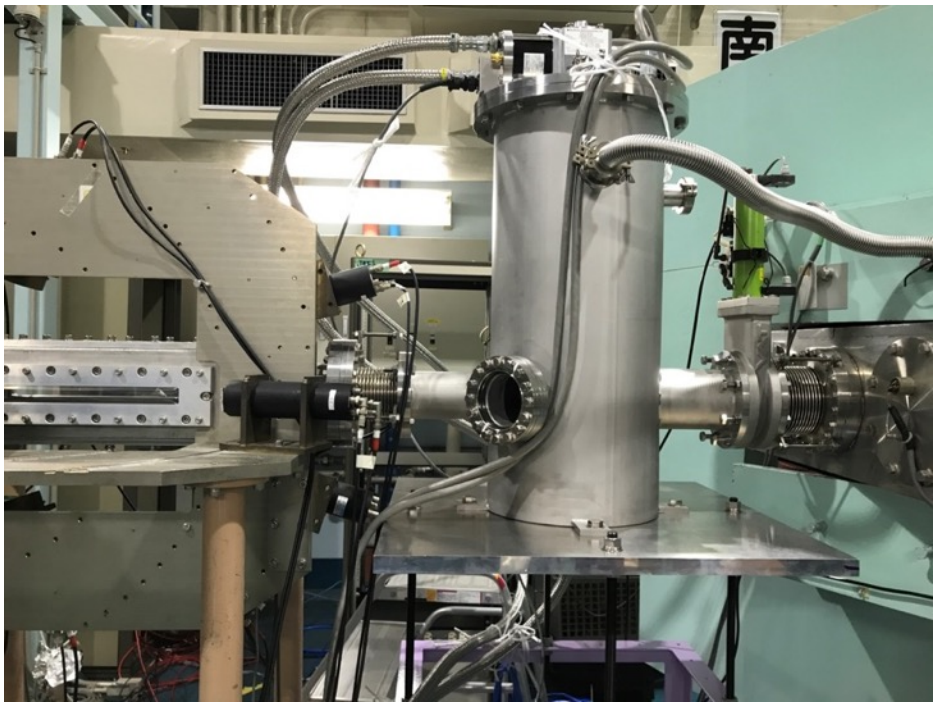

Fig. 5: View of experimental set up at RCNP for 200 MeV. The beam was introduced from left hand to right hand.

1.5 Measurement of displacement cross-section at 3-GeV synchrotron in J-PARC

A schematic drawing of experimental arrangement is illustrated in Fig. 6, which is utilized similar experiment carried out 3-GeV synchrotron in J-PARC. The chamber has

a movable stage to avoid unwanted beam irradiation since the proton beam introduced to the spallation neutron source passes the chamber. Due to the less space remaining around the beam dump, the vacuum chamber for the experiment shown in Fig. 6 cannot be placed to the beamline in front of beam dump. The chamber was placed at the upstream of the beam dump, where the high-intensity beam (1 MW) was transported to the spallation neutron source placed at the MLF. In order to avoid the melting the sample and the beam loss due to the high-intensity beam, a revision of the interlock system related to the radiation safety and Personnel Protection System (PPS) was required for the experiment.

To perform this experiment, we added the interlock that the sample could not move to the irradiation position when the beam destination was selected to the MLF. Therefore, a change of license of radiation safety is required to the experiment at 3-GeV beam dump. In summer outage 2017, the vacuum chamber shown in Fig. 7 was installed at the exit channel of the 3-GeV synchrotron. Since the license is not approved, the moving stage is physically fixed. After authorization of the new license, the experiment will hopefully start in this Japanese fiscal year.

It should be noted that detail safety assessments were required when the experiment was intensely discussed with the safety team in J-PARC. As one of the examples of risk assessment, detail thermal analysis of the sample and window were made, which is shown in Fig. 8. It was confirmed that the maximum temperature was about 100℃ and sample is not melted by malfunctioned GM cooler and introduced the maximum intensity of the beam to the dump, which was ~80 times higher of the beam planned in this experiment. Also, thermal stress and radiation safety were analyzed under the severe conditions, which are allowed by the interlock. Proposal of the experiment was submitted to the program committee in the MLF and was approved.

By changing the timing of extraction kicker magnet for the 3-GeV synchrotron, the kinematic energy of the extracted proton can be varied. It may allow us wide range of projectile energies from injection energy to synchrotron (0.4 GeV) to the maximum accelerated energy of 3 GeV. With gathering experimental results described above the experimental displacement cross-section will be obtained by an extended the energy range from 125 MeV to 3 GeV. However, in order to estimate the damage in the energy region higher than 3 GeV, the data in higher energy region are required. At least to understand the damage of the beam window used at T2K, the data for 30 GeV is

required.

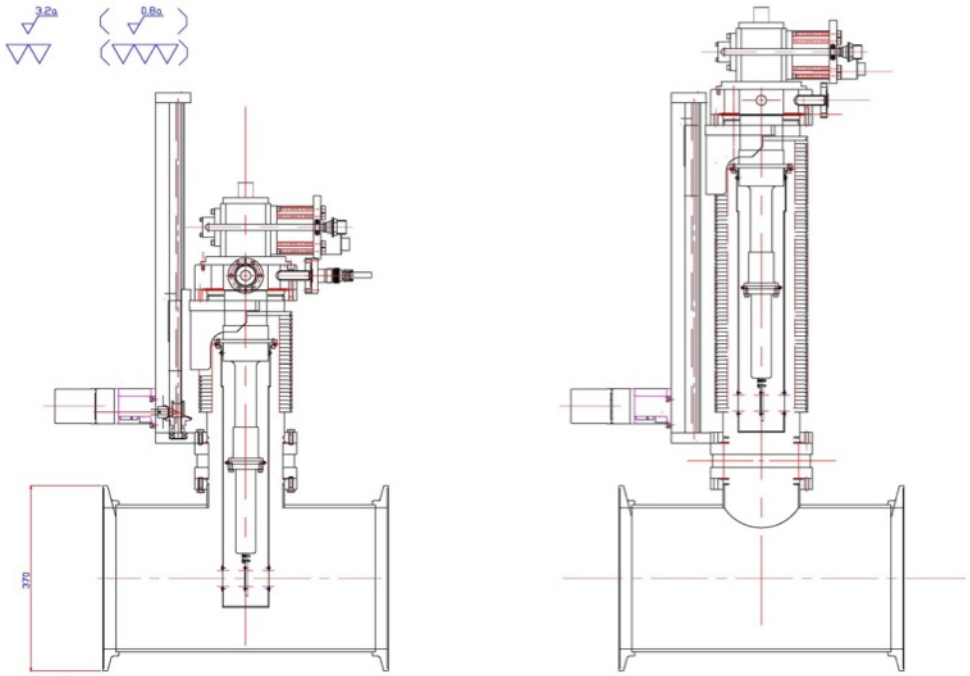

Fig. 6: Drawing of vacuum chamber placed at beam transport to 3-GeV beam dump, which has movable stage attaching the sample. Left-hand and right-hand side show position for irradiation and evacuation, respectively.

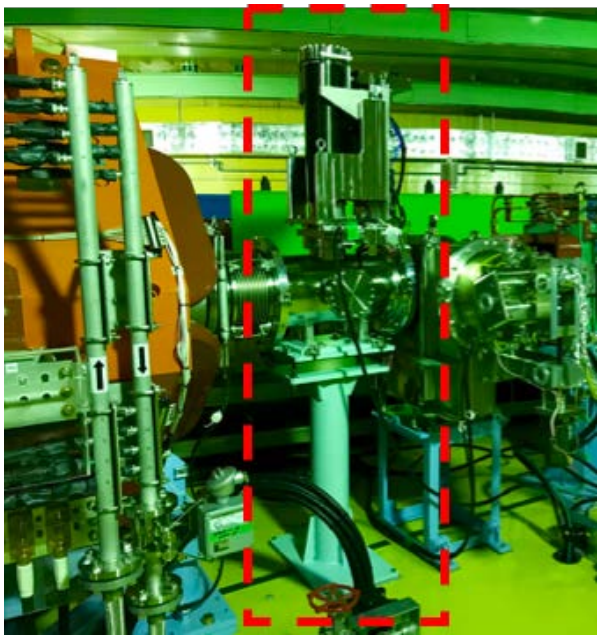

Fig. 7: Experimental chamber placed at 3-GeV proton beam transport.

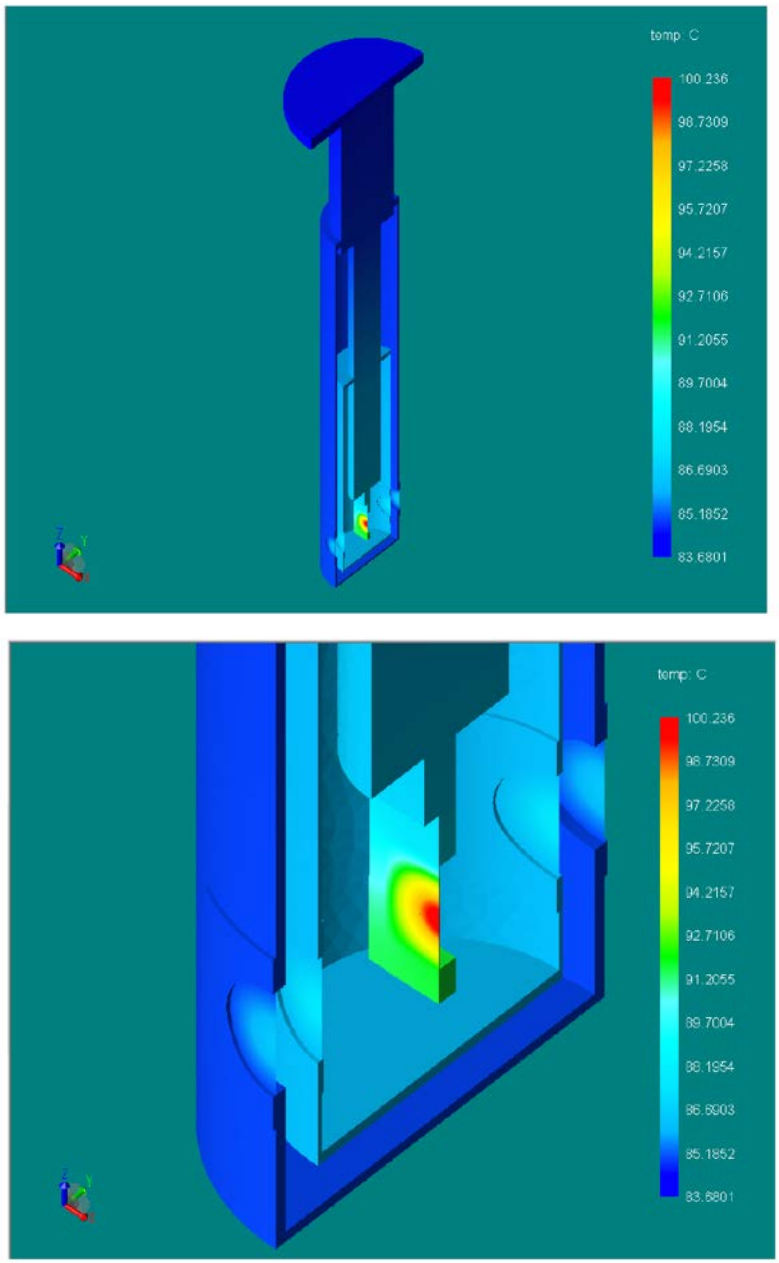

Fig. 8: Thermal analysis for the experiment carried out at 3-GeV synchrotron.

1.6 Expected results and their significance

The expected result is to produce the experimental displacement cross-sections of materials for validation of radiation damage models in PHITS which will be used for the design of J-PARC TEF (400 MeV) and ADS design (~1 GeV). The experimental data will also be utilized for the coordinated research project (CRP) in International Atomic Energy Agency (IAEA) titled with “Primary Radiation Damage Cross-sections” [20]. One of expected CRP outputs is to produce a digital database for displacement cross-sections of materials in the accelerator facilities. In the 2nd CRP meeting in June 2015, the CRP members suggested that our measurement data are essential to evaluate the displacement cross-sections because of no experimental data from 1 MeV to 1 GeV and no activity of this measurement except for us all over the world. They highly recommended us to continue the measurements.

After proton irradiations, the cryogenic device can also measure the thermal recovery of the radiation-induced resistivity increase using an electric heater. This data is required for the design of the superconducting magnet used in accelerator facilities. We found that the behavior of the resistivity recovery for 125 MeV protons is similar to that for 0.54 MeV protons, while 20% of the defects remain at an annealing temperature of 290 K. As there are no data on thermal recovery of radiation defects, our experimental data are also valuable for the design of superconducting magnet in accelerator facilities. In summary of the workshop of radiation effects in superconducting magnet materials held in FRIB Michigan State University in 2015 [21], it was recommended to carry out cryogenic irradiation measurements on metals employed as a superconducting magnet.

At neutrino facilities such as MINOS and T2K, beam windows such as beryllium and titanium alloy are employed. Under Radiation Damage In Accelerator Target Environments (RaDIATE) collaboration [22], the post-irradiation examination (PIE) was performed after irradiation of 181-MeV protons at Brookhaven Linac Isotope Producer (BLIP) in Brookhaven National Laboratory (BNL). In order to understand the change of mechanical properties for the window materials correctly, the accurate displacement cross-section is essential. Because the kinematic energy of proton used at BLIP is different from the actual projectile energy utilized in neutrino facilities, RaDIATE recommended performing the proposed experiment [23]. It can be expected

that the present experiment will contribute the safety and robustness of windows utilized at neutrino facilities in the world.

At LHC in CERN, superconducting magnets are utilized. With increasing power of the beam in the future upgrade plan at LHC, degradation of superconductors due to the radiation is one of the critical issues. Obtaining the data of the degradation of superconductors is essential. In the proposed experiment, the change of resistivity is directly observed under the cryogenic condition. The obtained data will help to recognize the degradation of superconducting magnets. Under Radiation Effects in Superconducting Magnet Materials 2017 (RESMM'17) [24], the experimental data was required.

2. Proposed experiment

2.1 Experiment at MR

2.1.1 MR abort beam dump

The beam transport to the MR abort line is shown in Fig. 9. With the bipolar kicker magnet, the beam is extracted from the MR and introduced to the dump beside the beam is kicked reverse direction to deriver T2K. We are planning the experiment with the beam introduced to the MR abort beam dump. After discussions with MR group, three candidate positions were chosen, where the experiment will be carried out as shown in Fig. 9. Since the GM cooler utilized in the experiment requires to be operated in the low magnetic field, we decided to be installed around position 3 expected lower field. Also, because of the requirement of the space for changing the sample, upstream position is not appropriate. In Fig. 9, a view around position 3 is shown, where an extinction monitor has been already installed, which had a vacant vacuum port to fit our GM cooler. We thought that our sample with GM cooler could be installed at the unused port. However, it was declined by the extinction monitor group because they will use in the future experiment that port. Therefore, we decided to install the chamber between candidate position of 2 and 3. With certain conditions such as avoiding interference the maintenance position for the MR, the use of the position was granted by the MR group.

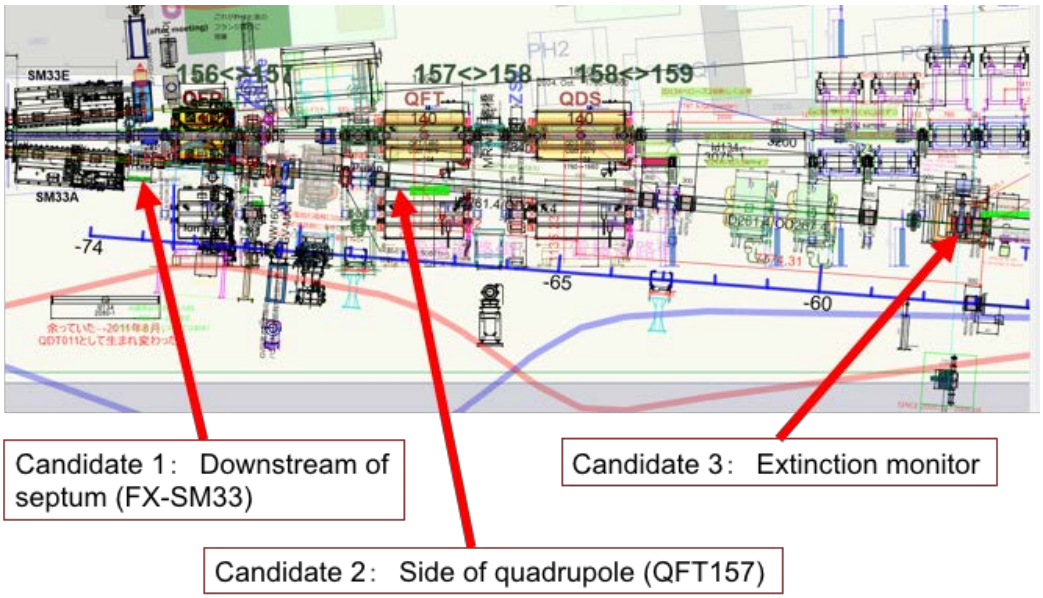

Fig. 9: Schematic of the MR abort beamline with the position of the candidates for the present experiment.

Fig. 10: Present view of candidate position 3 from upstream to downstream. Following quadrupole magnets (yellow), the chamber of the extinction monitor at candidate position 3 is shown.

2.1.2 Beam width at sample

Table 1 shows the beam width given by the MR group at the sample positions, where the experiment will be performed. In Table 1, also the widths for the kinematic proton energies 8 and 30 GeV with MR operation of the fast extraction (FX) and the slow extraction (SX) are shown. The position of the experimental chamber will be expected to be placed at upstream of position 3. As shown in Table 1, the beam width increases along to beam direction. For the temperature of the sample described in Section 3.2, the minimum size shown in Table 1 was employed. In the analysis of the radiation safety described in Section Beam loss3.3.1, the maximum size at position 3 was utilized to conservative estimation.

Table 1: Beamwidth of at candidate position at MR abort dump given by MR group.

Candidate	FX				SX			
position	8 GeV		30 GeV		8 GeV		30 GeV	
	σ_h [mm]	σ_v [mm]	σ_h [mm]	σ_v [mm]	σ_h [mm]	σ_v [mm]	σ_h [mm]	σ_v [mm]
1	11.04	0.76	5.97	0.42	10.72	4.23	5.80	2.27
2	14.99	5.21	8.10	2.79	15.73	4.95	8.44	2.65
3	20.46	12.88	12.49	6.58	22.52	11.02	13.66	5.64

2.1.3 Vacuum chamber for the experiment

One of the candidates of target chamber is shown in Fig. 11. To achieve a low temperature at the sample, the chamber has thermal shield surrounding the sample which will be attached first and second stage of the GM cryocooler. In this experiment, the observation of the beam profile is an essential. To obtain beam profile at the target position, the wires will be separated each position for horizontal and vertical direction. By observing the resistivity or temperature, the beam observes may be obtained, which is suitable for the FX. In order to minimize beam loss, the thermal shield and sample holder have a large aperture. The thin aluminum foil will be placed to decrease rising the temperature.

To make a physical boundary, the chamber has a vacuum gate valve, which allows exchange the sample during short outage after the sample moved to the evacuation position with a purged vacuum. After discussion MR group, moving direction of the sample was determined to have a vertical direction to avoid interference of the space for the maintenance the MR. The GM cooler coupled with the sample is thought to weight 60 kg so that a crane will be needed to exchange of the sample. At the candidate position 3, the crane placed in MR tunnel cannot reach the top of the chamber. Probably, a hoist mounted on the frame will be tentatively placed during sample exchange.

It should be mentioned that in the safety advisory committee for the experiment of the displacement cross-section at the 3-GeV synchrotron, it was pointed out that the movable stage for the sample should measure to the mechanical anomaly and the malfunction of its control system. The similar malfunction may occur during the experiment at the MR abort dump. Therefore, the manual function to evacuate the sample by human hands operation is installed in the present chamber as well. Also, the position indicator of the sample will be installed to the present chamber to recognize the position correctly. The vacuum chamber has viewports to observe the status of the thermal shield and aluminum window.

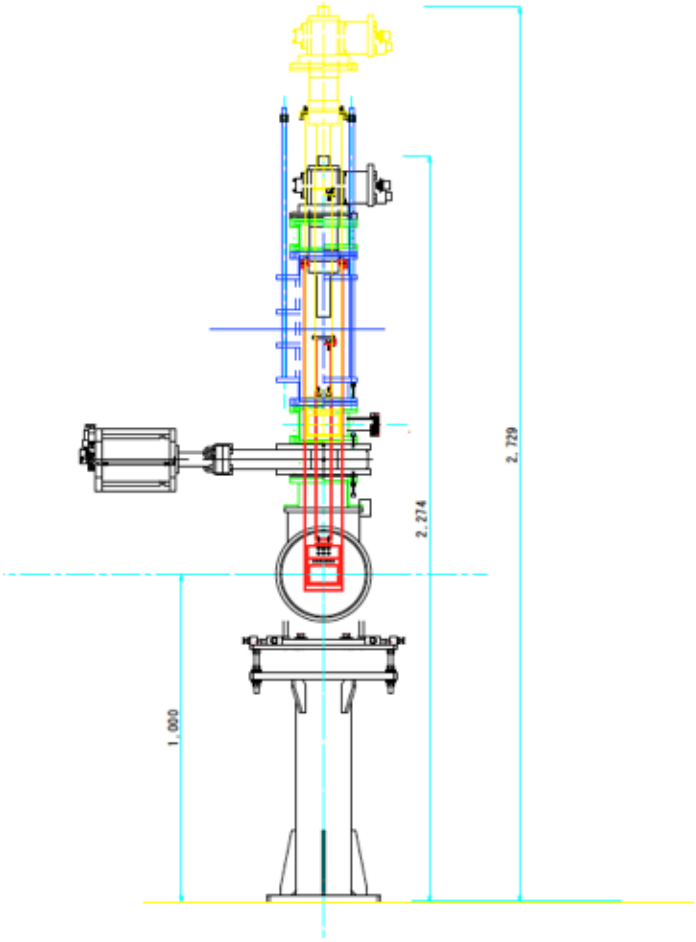

Fig. 11: Schematic drawing of the chamber at MR abort dump indicating for both irradiation and evacuation positions.

2.1.4 Required amount of protons for the present experiment

To make clear the experimental condition, let us discuss the experimental result with 125-MeV protons and 1 nA at the KURRI. In Fig. 12, the trend of the resistance of the copper sample (red line) and the temperature observed at the sample holder (blue line) is shown. At the KURRI, the exposure of three sets for 8 hours was applied. Since the temperature rising at the due to the heat is given by the beam, the resistance was rapidly increased. On the contrary, the resistance decreased immediately at the beam stop. With the beam irradiation with 1 nA for 8 hours, the resistance increased about 0.7 $\mu\Omega$. Although three times of irradiation was applied in the KURRI experiment, one set of irradiation for 8 hours having the amount of protons as 5×10^{14} is thought to be enough

to measure the displacement cross-section. Therefore, the number of incident protons for the experiment was decided to be 5×10^{14}.

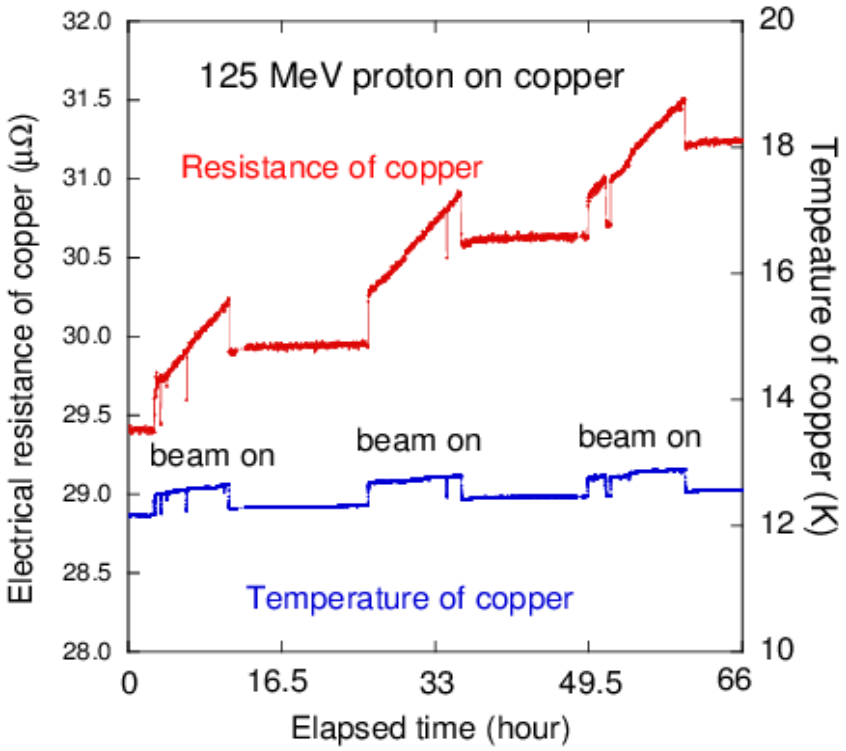

Fig. 12: Electrical resistance and temperature of the sample (Cu) during beam irradiation by 125-MeV with 1 nA protons carried out at KURRI [13].

At the KURRI experiment after the beam irradiation, the sample was annealed to observe reconvention of a vacancy in the sample depending on the sample temperature. Figure 12 shows the change of resistivity after beam irradiation with annealing. From this result, it was confirmed that the reconvention effect was small at the temperature around 13 K during beam irradiation. In Fig. 13, it was found that the mitigation of defect is gradually increased above 30 K so that the temperature should sustain by the adjustment of the beam intensity to obtain the cross-section with reasonable accuracy. It should be noted that the goal of accuracy obtained by the proposed experiment is now under discussion. Temperature is one of a critical issue for the accuracy. If the experiment was carried out using 5×10^{14} is for the duration of say 1 hour, the beam power was 670 W and the temperature rising was less than 10 K. We decided that case is a primary standard for the current experiment.

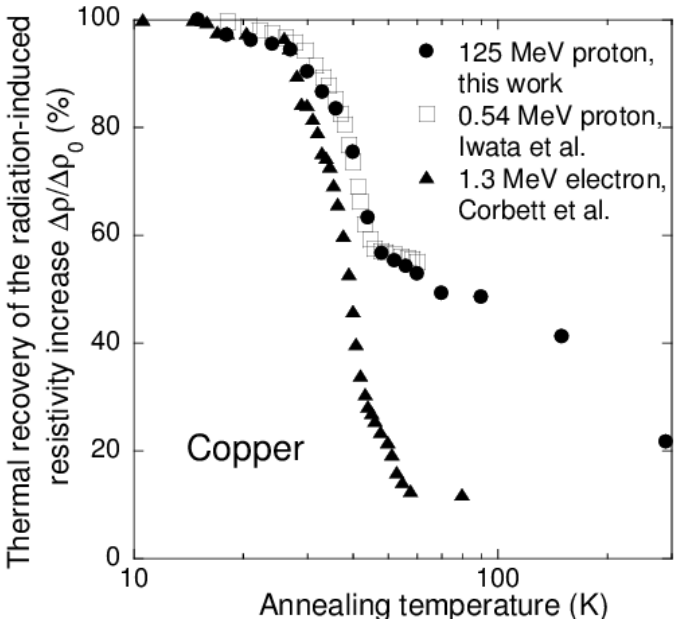

Fig. 13: Annealing temperature and thermal recovery of radiation-induced resistivity observed at KURRI experiment (circle) with other experiments (open square and triangle) [13].

For measurement of the electric resistivity increase under cryogenic irradiation, we will use the same manner with the experiment at KURRI and RCNP. Table 1 shows the estimated resistance increase of Al, W and Cu wires for the proposed experiment given by Eq. (3), in which displacement cross-section was calculated with PHITS. The sample wire will have a dimension of 13-cm length and 0.2-mm diameter. It is assumed that damage rate, $\Delta\rho_{metal}/\phi$ (resistivity change per beam intensity), is not so changed within beam area of 20 mm in diameter on the sample at the BNL and KURRI experiments because the BNL experiment indicated that resistivity increase of sample is proportional to beam intensity [6].

In the proposed experiment, the total amount of 5×10^{14} protons, which has an equivalent amount of protons with a beam power of 670 W with the kinematic energy of 30 GeV and irradiation duration of 1 h, introduce to the sample. Sustain the sample at low temperature is essential to remain the damage caused by proton. Beam current will be chosen in the intensity range lower than 1×10^{13} protons per shot, which will be adjusted to keep the low temperature in the sample. For each run of the experiment, the amount of the proton is required to 5×10^{14}. The duration of each run is expected as

much as 1 hour, which allows us the flexibility of beam time coupled. Samples of aluminum, tungsten, and copper will be utilized in this experiment. The samples will be changed during outage period so as not to disturb another experiment carried out at neutrino and hadron facilities.

Table 2: Estimated resistance increase of Al, W and Cu target using Eq. (3) and displacement cross-section calculated with PHITS.

Sample	Electric resistance at 6 K ($\mu\Omega$)	Frenkel pair resistivity ρ_{FP} ($\mu\Omega$m)	Expected displacement cross-section ($\times 10^{-25}$ m^2)	Accumulated beam flux at sample ($\times 10^{19}$/m^2)	Estimated increase in resistance ($\mu\Omega$)
Al	137	3.7	0.2	1.78	4
W	9700	27.5	2	1.78	292
Cu	29.4	2	1	1.78	11

3. Safety analysis of experiment

3.2 Thermal analysis

The temperature of the samples was estimated with the scaling of the 3-GeV beam dump result shown in Fig. 14. To accept wide beam introduce to the position 3, large aperture sample holder was utilized with 90 mm by 50 mm, in horizontal and vertical direction, respectively. In the analysis, tungsten sample was employed since the tungsten produces the most significant heat deposition than other samples. The result of the severe case without cooling cryogenic to measure malfunction of the cooling and was for 0.4 GeV giving highest heat deposition in the energy region for the 3-GeV beam dump. In the thermal analysis for the 3-GeV beam dump, following calculation heat density with PHITS finite element method (FEM) with the simplified geometrical model shown in Fig. 14. By scaling the heat deposition and the intensity, the present experiment case was made. The maximum temperature is shown in Table 3 for 30 GeV giving higher heat than 8 GeV. It is shown that the maximum temperature of the sample is less than 300℃ being lower than the melting point of aluminum (660℃), which has the lowest melting point of the samples. It may happen that the maximum beam power such as 1 MW may be introduced to the sample due to malfunction of the accelerator. Even in that case, the temperature of the sample, however, will rise several tenth ℃ so that the sample remains a solid state. Therefore, it can be concluded that the sample will not melt in this experiment.

Table 3 Maximum temperature of the samples irradiated with 30 GeV protons.

Proton energy [GeV]	**Al [℃]**	**Cu [℃]**	**Ti [℃]**	**Nb [℃]**	**W [℃]**
30	< 90	< 230	< 240	< 260	300
Melting point	660	1085	1675	1455	3422

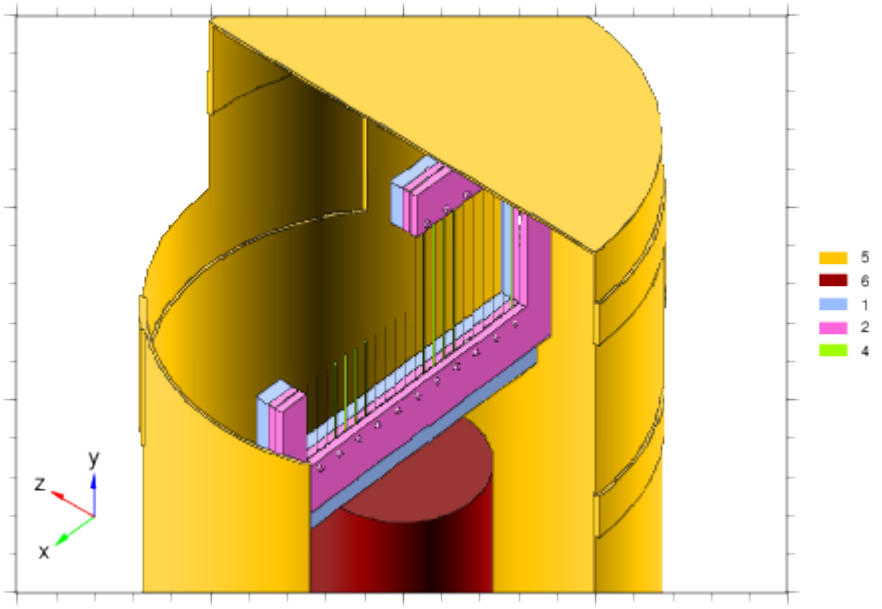

Fig. 14: Geometrical model employed for analysis of thermal and radiation.

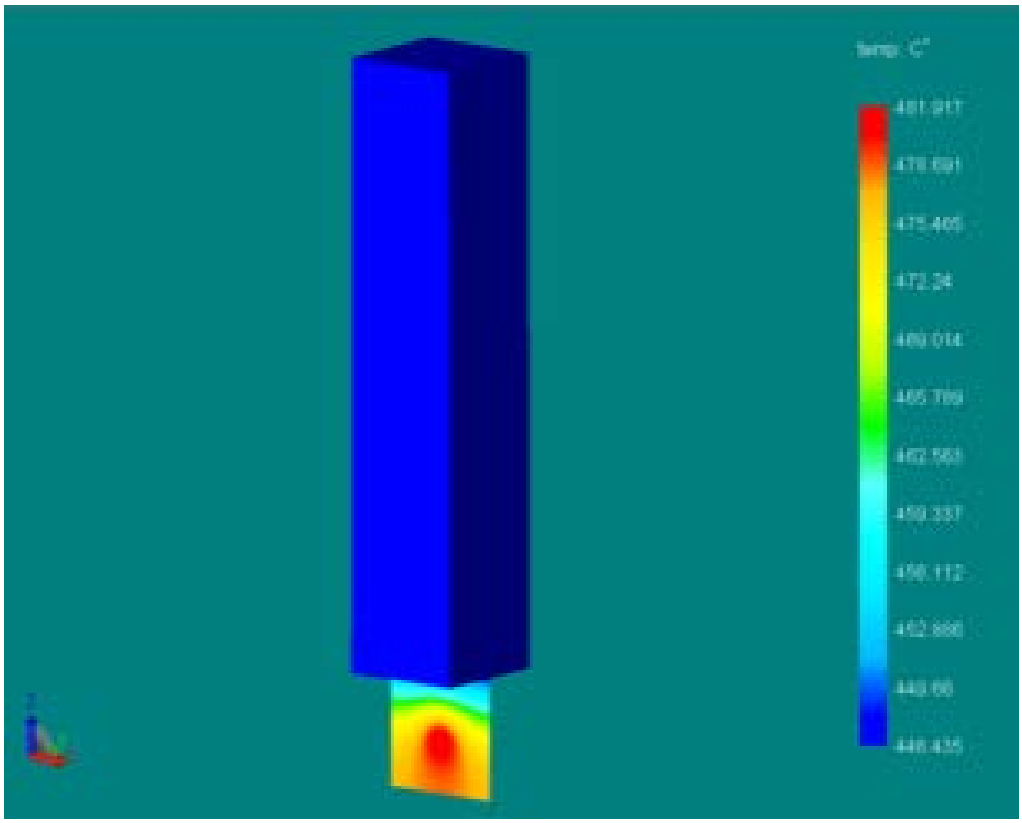

Fig. 15: Thermal analysis with simplified geometry for 0.4 GeV protons for the extremely severe case. Based on this result, the maximum temperature was estimated by scaling with the proton intensity and heat deposition obtained with PHITS.

3.3 Survey of radiation safety

3.3.1 Beam loss due to interaction

Radiation was evaluated with the calculation with PHITS. The beam loss due to the proposed experiment was obtained for the maximum beam intensity to the MR abort dump, which has the beam power of 7.5 kW. It was shown that the beam loss was 2.9 and 2.3 W for 0.8 and 30 GeV protons, respectively. In the present license, the line loss along the ring is determined as lower as 0.5 W/m, which is equivalent to point loss of 3.7 W at each quadrupole magnet. Furthermore, the licensee determined to the point loss at the extraction septum as 720 W. In this experiment, the beam power will be utilized about 670 W for 30 GeV, which is one and three magnitudes smaller than the maximum intensity to the MR beam dump and the T2K, respectively. From the result of the sample temperature and the beam loss, it can be concluded that the additional interlock is not required for the proposed experiment.

It should be noted that the beam power for the experiment will be limited less than 670 W to be kept the sample lower temperature for the conservation of the damage so that the actual beam loss will be 0.26 and 0.21 W for the proton beam of 0.8 and 30 GeV, respectively.

3.3.2 Radiation during beam irradiation

Figure 15 shows the flux distribution for all species particles. Since the beam loss is smaller than the value described in the license, flux is smaller than the allowable value. It should be mentioned that the helium compressor unit of the GM cryocooler has a control unit. Since the length of the horse for the helium gas is 60 m at maximum, the compressor had to be placed in the MR tunnel. The radiation hardness of the control unit is not apparent. Malfunction of GM cooler by the radiation may occur during beam operation. If the malfunction happened, although the experiment cannot be carried out as scheduled, it does not disturb the beam delivery to the T2K and hadron facility.

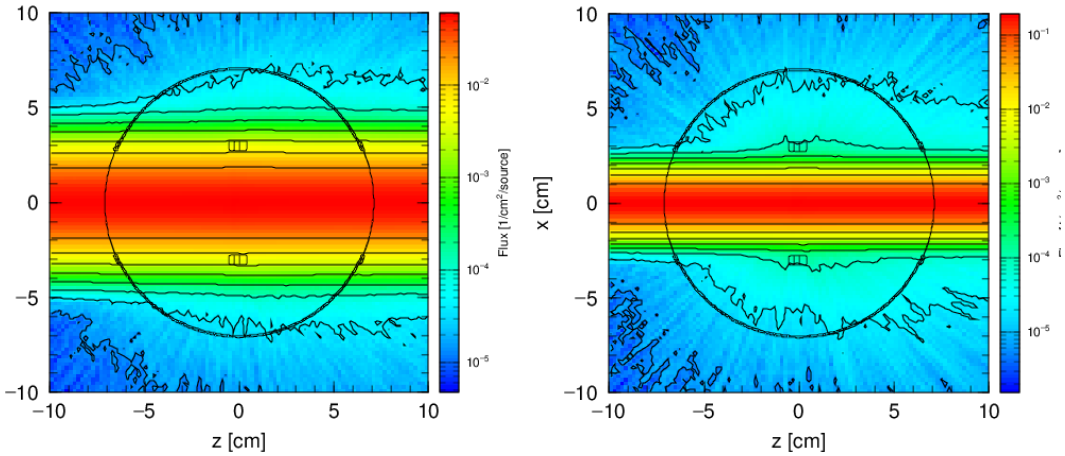

Fig. 16: Particle flux analysis during irradiation for 8 GeV and 30 GeV shown in the left and right-hand side, respectively.

3.3.3 Residual dose rate

The residual dose rate after beam irradiation was estimated by PHITS. With the geometrical calculation model shown in Fig. 6, the residual dose rate was estimated with the assumption that 6 times of beam time were allowed with the amount of protons of 5×10^{14} for each time. In the analysis, the calculation was made with the total amount of protons of 3×10^{15} introduced for negligible short time. Figure 17 shows the residual dose rate at 1 m for various decay time. In the analysis, the point source approximation was applied for simplification. The earliest access to the tunnel is limited to 4 hours of the beam operation.

In Table 4, the dose rate at 1m obtained with the calculation is summarized for various decay time. For the maintenance of the chamber, the worker typically will stay about 30 cm from the center of the chamber. In that case, the dose rate is about 10 times of the values shown in Table 1. Therefore, the maximum dose rate of working circumstance is estimated to be 79 μSv/h. Although smaller kinematic energy with the same amount, the dose rate for 8 GeV was higher than one for 30 GeV, which is caused by the large beam size as shown in Fig. 18, Since the beam size of 8 GeV is more significant, the dose rate increases by the beam at the edge hitting on the structural material used in the chamber. In Fig. 17, the contribution of each material on the dose rate is described. Figure 17 shows that the beam duct dominates in the total. In the

calculation of radioactivity, the beam duct of 2 m length was utilized. The dose rate obtained with the point source approximation, which overestimates the value. In order to obtain correct dose rate distribution around the beam duct, the rate was estimated with approximation having a uniform distribution on the beam duct, which is shown in Fig. 18. With uniform approximation distribution, the dose rate around the beam duct drastically was decreased to 3 μSv/h. The distribution of radioactivity in the duct is thought to be localized around the sample so that the uniform approximation may underestimate the dose. The actual dose rate can be thought to lie on the value between two approximations. Therefore, it can be thought that the dose rate around at the duct is ~80 μSv/h including with the safety margin of factor 2. The exposure dose for the maintenance of the chamber and sample was expected to be less than 200 μSv/h during the work for 2 hours, which was at a reasonable level of dose for maintenance.

Exposure due to the inhalation was estimated as the result of radioactivity. In Fig. 19, the radioactivity of total equipment for the experiment except the beam duct is shown, which shows the main contribution of the activity is the sample. Since tritium cannot be removed easily, the estimation was made for the internal dose due to inhalation of the tritium. The total amount of the tritium was estimated ~10^4 Bq at the sample. The amount of inhalation dose was 1.8×10^{-5} times of the total activity of inhaled tritium. The internal dose was ~0.18 μSv even if the total tritium was halted to one person. Therefore, the dose due to inhalation of tritium can be concluded to be negligibly small.

Table 4: Estimated residual dose rate [μSv/h] with a distance of 1 m from the sample for each decay time after irradiation.

Decay time	**8 GeV**	**30 GeV**
4 hour	7.9	4.3
1 day	1.2	0.55
7 days	0.09	0.05
1 year	0.002	0.001

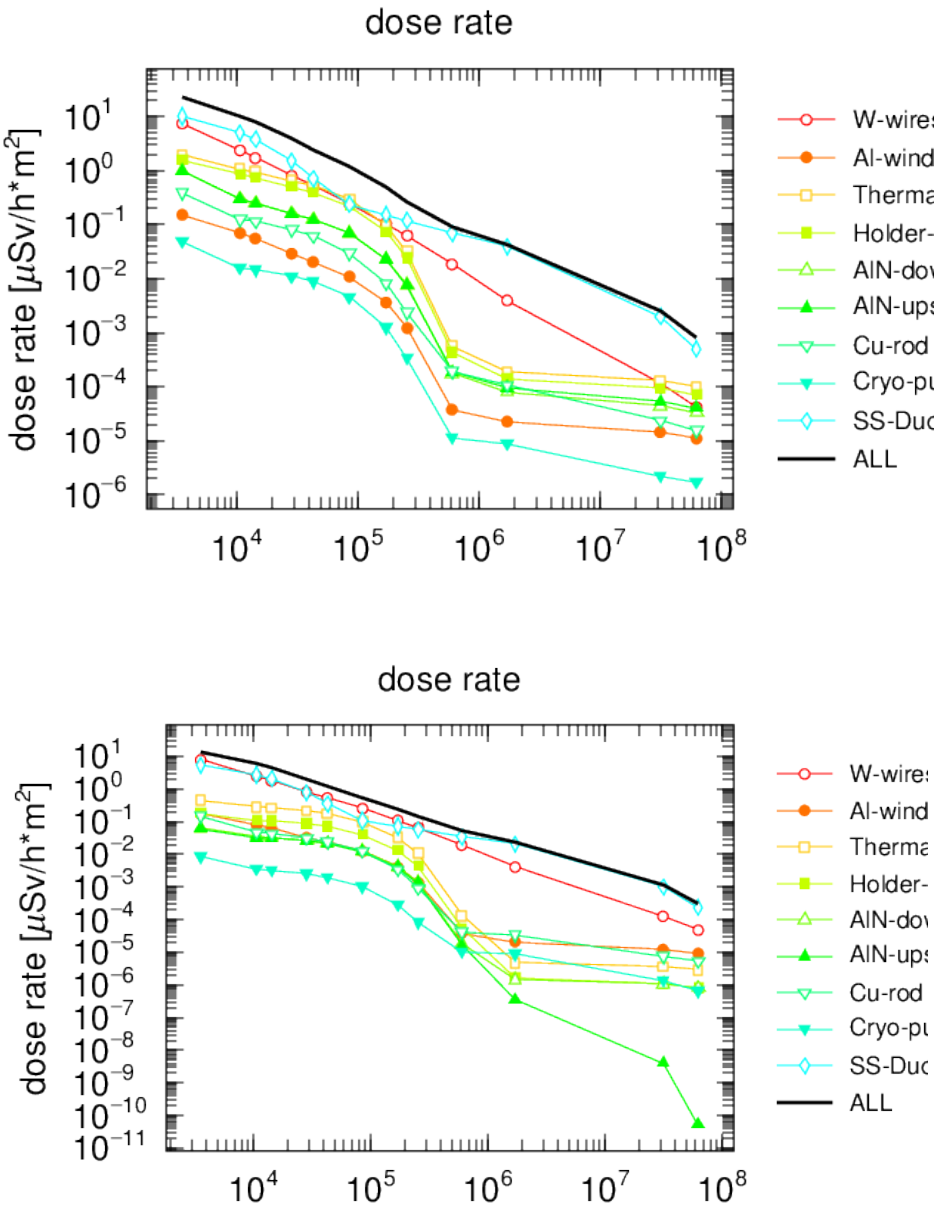

Fig. 17: Does rate at distance of 1m with approximation point source as a function of decay time for 8-GeV and 30-GeV protons shown in top and bottom, respectively.

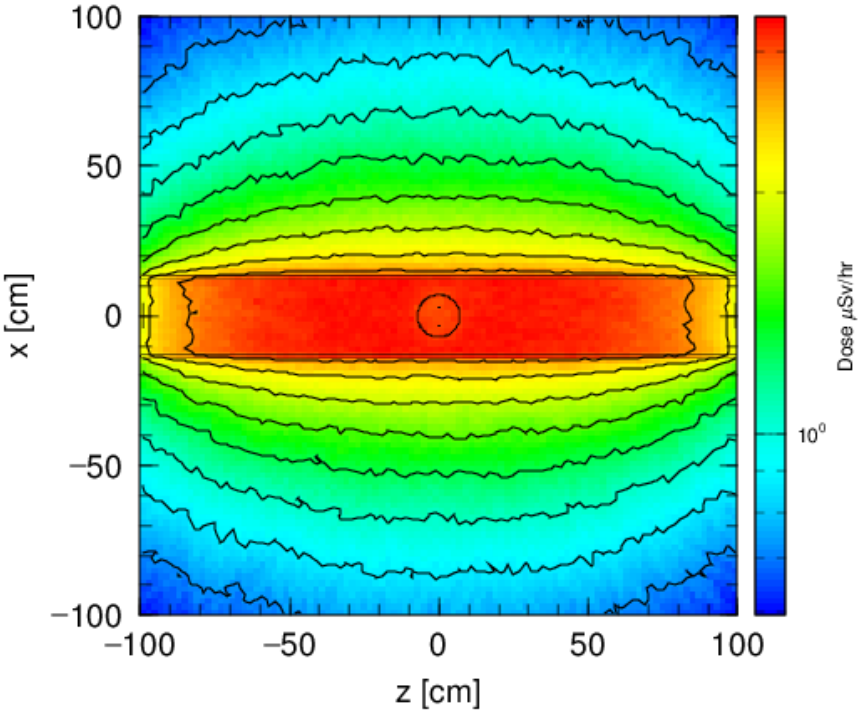

Fig. 18: Does rate distribution radiation for 30-GeV protons produced from the beam duct after 4 hours of decay time with the assumption of activated uniformly

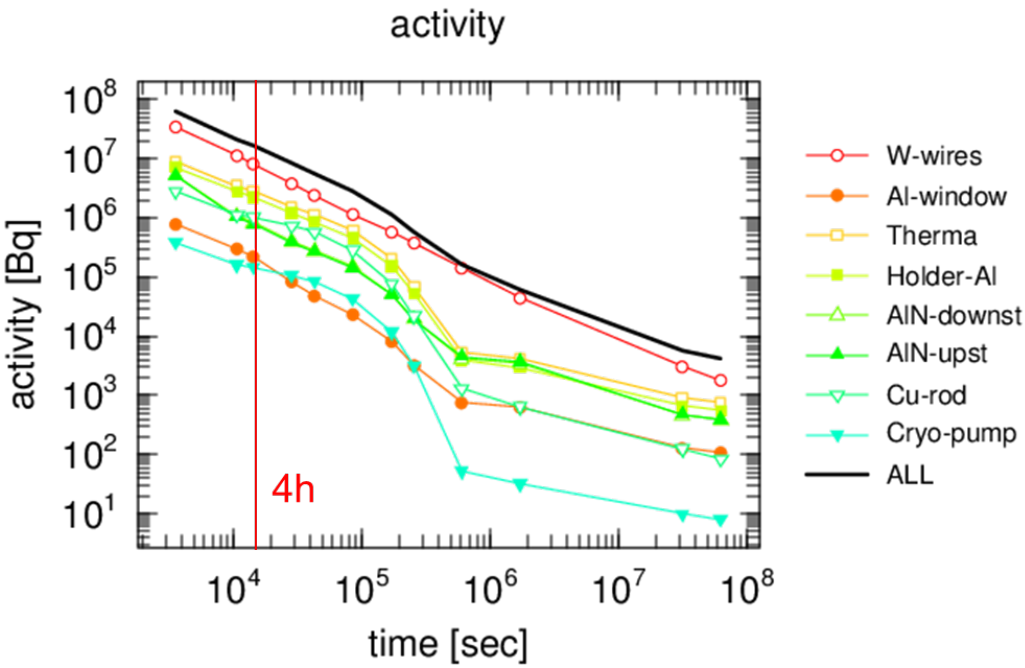

Fig. 19: Radioactivity of 8-GeV protons case. In the analysis, the calculation was made without beam duct made of stainless steel.

3.4 Malfunction of vacuum

The chamber has pneumatic gate vacuum valve shown in Fig. 11 to endure high radiation. To prevent malfunction event of vacuum, control will be required by the machine protection system (MPS). If abnormal vacuum pressure were found at the irradiation position, the sample would be moved to evacuation position immediately, and the vacuum valve will be closed for the isolation to the beamline. In J-PARC accelerator, the bellows were ruptured at the 3-GeV synchrotron of the beam collimator due to the malfunction of its control system. For the avoidance of the similar event, the physical block will be installed in the chamber to determine the movable range of the position.

It may happen that the rupture of the thinner aluminum window to be placed at the thermal shield during pumping of the sample coupled with the GM cooler. Before irradiation, the sample will be pumped through a closing gate valve for the isolation of the beamline. In order to confirm the health of the window during pumping, a viewport will be installed to the evacuation position of the sample. After the pressure around the sample achieved low pressure, the valve can be opened to move the sample to the irradiation position.

3.5 Helium leak from GM cooler

As assessment of safety, the risk for the workers in the tunnel is estimated when the helium is leaked to the atmosphere during the maintenance period. The total amount of helium contained in GM cooler has a volume of 10 m^3 in ambient temperature at 0.1 MPa. Assuming the leaked helium stayed inside the cube having each flowing to a cube with each side length of 5 m (125m^3), the concentration of oxygen in the cube decreases to 19.3% from 21% due to the leakage. Since the lowest concentration limit 18% determined in the law, the concentration remains more substantial than the limit. The total volume of the MR tunnel is 60,000 m^3, which is as much as 480 times of the cube used in the estimation. Therefore, it can be concluded that the helium leakage event does not influence the workers inside the MR tunnel. During beam operation when the leakage happened, the pressure at the tunnel will increase. The increase in the pressure due to the leakage is tiny (17 Pa) so that the leakage does not issue in the viewpoint of

pressure control in the tunnel.

As for the leakage helium from the cooler to the vacuum, according to the vendor of the GM cooler, the failure of the cooler will not occur except the failure at welding at the vacuum part of the GM cooler. By the cooling test before installation to the beam line, the risk can be reduced. Furthermore, the impact on the beam operation delivering the beam to the T2K and hadron facility may be minimized by closing the isolation gate valve immediately by the pneumatic during the beam operation.

4. Experimental procedure

4.1 Schedule

The GM cooler and measurements device were already procured. In next fiscal year, cooling test using the GM cooler and a test chamber will be carried out. After discussion with the MR group, the detail design of the chamber will be fixed in this fiscal year. Due to the budget profile changed by the MEXT, all equipment required for the experiment cannot be procured in the next fiscal year. The rest of equipment and install will be completed by the summer of 2019.

After approved the present proposal by the PAC, the target chamber will be installed during summer outage in 2019. The safety group may require a minor change of the license such as the aim of facility use. If the revision of license were required, new license coupled with another modification required in J-PARC would be discussed and fixed by the safety committee in J-PARC, likely it will continue up to summer 2019. The modified license will be expected to be granted by autumn 2019. The experiment will be prospectively carried out in from Japanese fiscal year (JFY) 2019 to 2020. Following the research plan granted by MEXT, the present experiment will run up to the end of JFY 2019 March 2020. We hope that the experiment will start from December 2019 and continue to the end of March 2020.

4.2 Procedure for the experiment

4.2.1 Preparation of experiment

In this experiment protons with the kinematic energy of 8 and 30 GeV will be introduced to the sample. COMET experiment uses the 8 GeV protons so that 8 GeV proton is essential for the present experiment. Compressor for the GM cryocooler will be placed in the MR beam tunnel due to the length of helium supply, which is limited less than 60 m.

After the present proposal approved, the chamber will be installed in the MR tunnel. Our group will install the chamber with the association of the MR group. In the

experiment, after beam tuning by the MR group, the resistivity and temperature will be measured by us. After irradiation, the sample will be evacuated from the beam, and the resistivity by annealing will be measured.

4.2.2 Beam tuning

Before the cryogenic irradiation on the sample, characteristic of the beam will be measured by beam monitors placed at MR to obtain the beam profile at the sample, which will be probably carried out following to beam study at MR. Duration of beam tuning is expected to 30 min.

In the experiment, the sample will be utilized having separation wires. By observing the rising of temperature, the beam profile can be obtained. For this sake, the wire will be stringed to both horizontal and vertical directions.

4.2.3 Irradiation

After beam tuning, the sample will be moved to the irradiation position. In order to perform irradiation efficiently, the status of beam irradiation such as proton amount per shot and accumulated proton power will be controlled by the MPS. Also, the MPS will be installed to control irradiation condition according to the sample position. Additional, control system will be made to avoid too much irradiation, which is already made for the experiment at the 3-GeV beam line based on the SAD [25]. A similar system can be utilized for control for the proposed experiment.

4.2.4 After irradiation

For the routine beam operation to deliver the beam to the T2K and hadron facility, the beam transport to MR aborts dump must be emptied for the abort due to the failure of the accelerator. Therefore, after irradiation, the sample must be retracted from beam irradiation position. After moving to the evacuation position, the thermal recovery of defects with annealing will be measured with the close of the vacuum valve.

4.2.5 Sample exchange

Samples of this experiment will be changed during short outage period, which will be taken every week. Because the reduction of outgassing from the new sample requires long duration, probably every two months at most frequent will take for outgassing the new samples.

4.3 Readiness

The budget of the present proposal has been already funded in the research program of “Measurement of displacement cross-section using J-PARC of structural material for Accelerator Driven System (ADS)” entrusted to Japan Atomic Energy Agency (JAEA) by the Ministry of education, culture, sports science, and technology Japan (MEXT). All the equipment for the present experiment is procured by KEK, whose budget is given by JAEA as entrusted research. In last year, the GM cryocooler, DC power supplies and voltage meter for resistivity measurement, and the thermometer had procured. In this fiscal year, moveable stage and a vacuum chamber for the cryogenic will be finished procurement. In the next fiscal year, all-metal gate valve and parts of the chamber will be procured. In JFY 2020, the whole of procurement will be completed and will be installed in the MR tunnel.

We have been already installed the experimental chamber at the 3-GeV synchrotron with changing interlock system and radiation safety license. The proposed experiment is not required changing the interlock system of license as mentioned in section 3.3.1. Although the proposed experiment might be required to be changed the aim of the facility described in the license, it will be minor work such as changing the word in license and soon be granted by the authority of radiation.

We have been carried out a similar experiment at KURRI and RCNP. In J-PARC, the similar experiment will begin at the 3-GeV synchrotron. Some of us are the expertise of the cryogenic system and are the expertise of the beam dynamics and control system. By gathering our knowledge and experiences, it can be expected that the proposed experiment will be carried out smoothly.

4.4 Request for beam time

Request of the beam time for the proposed experiment is summarized in Table 5. In this experiment, the proton with the kinetic energy of 8 and 30 GeV will be introduced to the sample. Up to now, 8-GeV proton beam has not been transported to the dump. It is expected that the transport will be demonstrated in early 2020.

In JFY 2019, the chamber will be installed to the MR tunnel in the summer outage. We expected that the first experiment for 30 GeV would start by the end of 2019. Until the end of JFY 2019, we expected to experiment with 8-GeV protons. In JFY 2020, four times of beam time will be required to extend the data according to the mass dependence of nuclide from copper to tungsten. It should be noted that we may request extend the period of the experiment if the failure of the accelerator.

After finishing a series of experiments, the chamber with the movable stage will remain at the MR tunnel, which can be utilized another study such as the development of the beam monitor. The GM cooler will be extracted from the chamber to prevent beam irradiation. The GM cooler can be for another study such as the development of the beam monitors with cryogenic. Since the GM cooler has activation, the cooler will be limited to use in the radiation control area.

Table 5: Requirement of the beam time for the proposed experiment.

Fiscal year	Requirement of time experiment
2019	2
2020	4

5. Summary

To obtain displacement cross-section, we propose the experiment using the 8 and 30 GeV protons by placing the experimental chamber at the MR beam dump. Using the results obtained by the present experiment, the damage estimation for the target and beam window material can be improved. Since the current experiment directly observes the resistive change at the cryogenic due to the radiation, the result of the present experiment will contribute to improving the estimation on the degradation of the superconducting magnet with high-radiation circumstance such as the upgrade of the LHC.

It can be concluded that the safety of target at the high-intensity frontier will be improved by the present study. Although a minor risk such as rupture of bellows at the vacuum chamber, of which almost vacuum equipment placed at MR has, may increase due to the present experiment, however, we firmly believe that the overall risk such as a rupture of target, window and the failure of superconducting magnet can mitigate by the present work.

References

[1] D. Filges, F. Goldenbaum, Handbook of Spallation Research, Theory, Experiments and Applications, Wiley-VCH Verlag GmbH KGaA, Berlin, Germany, 2009. p. 215–232.

[2] N. Mokhov, V. Pronskikh, I Rakhno, S. Striganov, I. Tropin, MARS15 Developments Related to Beam-Induced Effects in Targets, 6th High-Power Targetry Workshop, Oxford, UK, April 11-15 (2016).

[3] M. J. Norgett, M. T. Robinson, I. M. Torrens, Nucl. Eng. Des. 33 (1975) 50–54.

[4] C. H. M. Broeders, A. Yu. Konobeyev, J. Nucl. Mater. 328 (2004) 197–214.

[5] C.H. Pyeon (Ed.), Current Status on Research and Development of Accelerator-Driven System and Nuclear Transmutation Technology in Asian Countries: KURRI-KR(CD)-40, 2013, ISSN 1349-7960.

[6] IFMIF International Team. An activity of the International Energy Agency (IEA) implementing agreement for a program of research and development on fusion materials. IFMIF comprehensive design Report;

[7] G.A. Greene, C.L. Snead, C.C. Finfrock, Jr., A.L. Hanson, M.R. James, W.F. Sommer, E.J. Pitcher, L.S. Waters, Direct measurements of displacement cross-sections in copper and tungsten under irradiation by 1.1-GeV and 1.94-GeV protons at 4.7 K, in: Proceedings of Sixth International Meeting on Nuclear Applications of Accelerator Technology (AccApp’03), Ja Grange Park, Illinois, USA, 2004, p.881–892.

[8] J.A. Horak, T.H. Blewitt, J. Nucl. Mater. 49 (1973/74) 161–180.

[9] P. Ehrhart, U. Schlagheck, J. Phys. F: Metal Phys. 4 (1974) 1575–1588.

[10] M.W. Guinan, J.H. Kinney, V. Konynenburg, J. Nucl. Mater. 133&134 (1985) 357–360.

[11] M.W. Guinan, J.H. Kinney, J. Nucl. Mater. 108&109 (1982) 95–103.

[12] Y. Ishi, M. Inoue, Y. Kuriyama, Y. Mori, T. Uesugi, J.B. Lagrange, T. Planche, M. Takashima, E. Yamakawa, H. Imazu, K. Okabe, I. Sakai, Y. Takahoko, Present status and future of FFAG at KURRI and the first ADS Experiment, in Proceedings of IPAC’10, Kyoto, Japan, 2010, p. 1327–1329.

[13] Y. Iwamoto, T. Yoshiie, M. Yoshida et al., J. Nucl. Mater. 458 (2015) 369–375.

[14] T. Sato, K. Niita, N. Matsuda, S. Hashimoto, Y. Iwamoto, S. Noda, T. Ogawa, H. Iwase, H. Nakashima, T. Fukahori, K. Okumura, T. Kai, S. Chiba, T. Furuta, L. Sihver, J. Nucl. Sci. Technol. 50 (2013) 913–923.

[15] Y. Iwamoto, K. Niita, T. Sawai, R.M. Ronningen, T. Baumann, Nucl. Instrum. Meth. B 274 (2012) 57–64.

[16] J.F. Ziegler, in: J.F. Ziegler, J.P. Biersack, U. Littmark (Eds.), The Stopping and Range of Ions in Solids, Pergamon Press, New York, 1985, http://www.srim.org/.

[17] B. Bordini, L. Bottura, L. Oberli, L. Rossi, E. Takala, IEEE Trans. Appl. Supercond. 22 (3) (2012) 4705804.

[18] L. Rossi, O. Bruning, High Luminosity Large Hadron Collider: A Description for the European Strategy Preparatory Group, CERN, Geneva, Switzerland, CERNATS- 2012-236, 2012.

[19] https://indico.cern.ch/event/282344/.

[20] https://www-nds.iaea.org/CRPdpa/

[21] https://indico.fnal.gov/conferenceDisplay.py?confId=8709

[22] https://radiate.fnal.gov

[23] https://conference-indico.kek.jp/indico/event/16/

[24] https://kds.kek.jp/indico/event/23554/

[25] http://acc-physics.kek.jp/SAD/